

We are IntechOpen, the world's leading publisher of Open Access books Built by scientists, for scientists

6,900

Open access books available

186,000

International authors and editors

200M

Downloads

Our authors are among the

154

Countries delivered to

TOP 1%

most cited scientists

12.2%

Contributors from top 500 universities



WEB OF SCIENCE™

Selection of our books indexed in the Book Citation Index
in Web of Science™ Core Collection (BKCI)

Interested in publishing with us?
Contact book.department@intechopen.com

Numbers displayed above are based on latest data collected.
For more information visit www.intechopen.com



Optical Methods Applied to Hydrodynamics of Cohesive Sediments

Juan Antonio Garcia Aragon,
Salinas Tapia Humberto, Diaz Palomarez Victor and
Klever Izquierdo Ayala

Additional information is available at the end of the chapter

<http://dx.doi.org/10.5772/intechopen.72347>

Abstract

Suspended sediment transport in large rivers is constituted mainly by cohesive sediments, which form aggregates or flocs with primary particles less than 65 μm . The removal of cohesive sediments in aquaculture tanks is a difficult problem. Due to its size, density, and shape, the hydrodynamic behavior of flocs is very different from that of non-cohesive sediments as they depend on the interaction with the water column. This chapter describes the experimental results obtained in sedimentation tanks, reduced models of aquaculture recirculation tanks, and a rotating circular flume with Plexiglas walls, in which optical methods were used to determine flocs' characteristics. These methods include particle tracking velocimetry (PTV) and digital holography for particle image velocimetry (DHPIV). Fractal models for floc density were successfully developed and validated with PTV experimental results in an aquaculture recirculation tank. Also, a model for the settling velocity of the flocs was validated using a permeable drag coefficient definition. Suspended sediments from Mexico's two largest rivers, Usumacinta and Grijalva, with a mean flow rate near mouth of 1700 and 650 m^3/s , respectively, were analyzed in a rotating circular flume. The shear velocity obtained in the field was reproduced in the circular flume and size and shape of flocs were obtained. This allowed to reproduce suspended sediment concentration profiles of rivers. DHPIV techniques were developed in order to obtain the actual size of the flocs based on Fresnel approximation for the reconstruction of holographic images.

Keywords: floc, settling velocity, suspended sediments, fractal dimension, PTV, DHPIV

1. Introduction

Hydrodynamic behavior of cohesive sediments is important in many fields of engineering. A large part of the suspended sediment charge in large rivers is constituted by cohesive sediments

as shown in the Amazon River sampling of suspended sediments [1]. A characteristic of cohesive sediments is to form aggregates (flocs) that behave in a very different way than non-cohesive sediments. Measuring *in-situ* flocs settling velocities in rivers is not possible with conventional sediment sampling instruments. Recently, *in-situ* optical instruments are being used for floc size measurement, particularly in the field of oceanography [2, 3]. Those instruments are very expensive because they use laser illumination and are not used in common river engineering practice. In this chapter, a method based on suspended concentration sampling and laboratory particle size analysis in a rotating annular flume is used to obtain flocs size, and with an appropriate settling velocity model deduce the settling velocity to be used in the Rouse equation. The method is validated with sediments from Usumacinta and Grijalva rivers, the two major rivers in México, whose basins are located in the states of Chiapas and Tabasco near the Guatemalan border.

The settling velocity of cohesive sediments is an important design parameter in aquatic environments such as water treatment plants, storm water ponds, sediment filling in lakes, sedimentation in estuaries, dredging in rivers, and sediment removal in aquaculture devices especially when shortage of water is a concern [4]. The reuse of water is the main characteristic of the latter systems.

The efficient removal of solids is a main concern in these systems because of the accumulation of non-used food and fish excreta. These solids are generally less than 65 μm in diameter and behave as cohesive sediments [5]. These sediments form flocs or aggregates, made of water, inorganic particles, and organic particles [6–8]. To obtain adequate settling models for these particles is an active field of research [9]. Some researchers include variable fractal dimension functions that depend on a characteristic size of flocs that is difficult to obtain over a large population of flocs [10]. Other authors use geometrical parameters of flocs like floc perimeter, which is not easy to measure in engineering practice [11, 12]. The flocs' settling velocity model proposed in this study uses parameters that are possible to average, using optical methods with some floc samples.

The tanks most widely used are circular [13, 14]. Water is supplied in these tanks by means of diffusers at the walls. In this project, a small scale circular water recirculation tank was used in order to study the solids behavior in the tank. There is a central settling device in order to remove the solids (**Figure 1**). The settling device functions according to the hydrocyclons principle [15].

Two optical techniques were used in this work, Particle Image Velocimetry (PIV) and Particle Tracking Velocimetry (PTV), to measure fluid and particle velocities, respectively. Polyamide tracers 25 μm in diameter were used to obtain fluid velocities using PIV, and flocs were tracked as particles in the PTV technique. PTV also allowed us to measure particle size and shape. Digital holography for particle image velocimetry (DHPIV) has also been used to determine the size and shape of flocs considering their volumetric nature.

The attempts to model settling velocity as a function of floc size, shape, and density demonstrated that density varies with floc size. Later work demonstrated that floc density depends on the fractal nature of flocs [16]. Recently, the effect of shear rate on floc density was demonstrated [11].

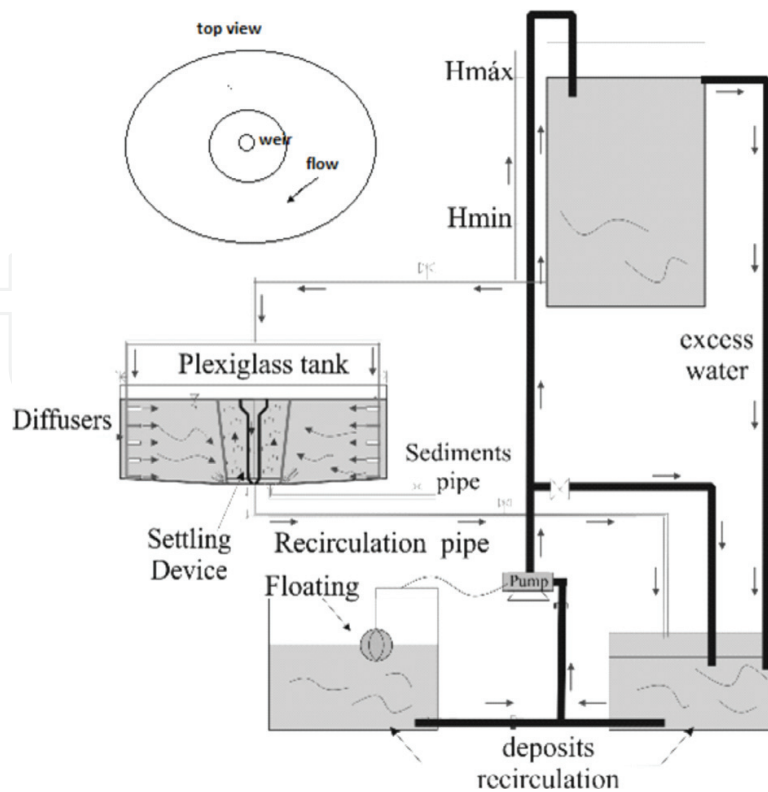


Figure 1. Reduced model of an aquaculture recirculation tank.

In this study, the results were used to calibrate settling velocity models using fractal theory and by including an adequate definition of the drag coefficient for permeable flocs. The proposed model is shown to provide reproducible results if a calibration of the parameters in the density vs. diameter model is properly done.

Suspended sediment samples obtained near the mouth of the Grijalva and Usumacinta rivers were analyzed in a rotating annular flume using PTV. It was possible to obtain appropriate values of the Rouse parameter Z_R , which was shown to be difficult to obtain with classical granulometric and Coulter counter methods used in river studies [1].

2. Methods

2.1. Experiments using PTV and sediments coming from aquaculture recirculation tanks

Initial experiments were performed with fish food in order to have a better control of primary particles. The sediments were sieved and only those passing sieve 200 (0.075 mm), with a mean density of 1430 kg/m^3 were used. A Plexiglas settling column was realized in order to allow the use of PIV and PTV optical methods. The set up consisted of a rectangular tank of cross section $15.5 \times 15.5 \text{ cm}$ and 100 cm height. A laser sheet was introduced from above using a double

pulsed Nd:Yag laser (15 mJ), high-speed CCD cameras JAI (250 fps and resolution and 1600×1400 pixels) were mounted laterally to the column and synchronized by means of a NI-PCIE-1430 card with laser pulses. Both cameras were equipped with 50 mm NIKKON lenses. The cohesive sediments were introduced manually and images were captured at the 30, 60, and 90 cm marks from the bottom of the tank. The resulting frequency histograms are presented in the following of the paper. For the processing of the images, the software used was PTV-SED v2.1, developed at CIRA to analyze the fall velocity of sedimentary particles in two-phase flows. PTV operation comprises of two sequential procedures. The first procedure implies improving image quality through spatial filtering. The second procedure implies detecting particles in each pulse following the five stages proposed: (i) identify maximum and minimum intensity (black or white) over the particle image to determine its size; (ii) from the intensity of pixels of the evaluated particle, a circular area is formed which can be used to determine the cross-sectional particle area (A), and then the equivalent diameter (d) can be estimated using $d = 2\sqrt{A/\pi}$; (iii) from the cross-sectional particle area (A) and pixel intensity, the coordinates (x, y) of the drop centroid are determined; (iv) pairs of double-pulsed particle are identified and the distance separating their centroids ($\Delta x, \Delta y$) is determined; and (v) Particle velocity (v_x, v_y) is obtained as follows:

$$(v_x, v_y) = \left(\frac{\Delta x}{\Delta t}, \frac{\Delta y}{\Delta t} \right) \quad (1)$$

Then a small scale water recirculation tank made of Plexiglas 35 cm in depth and with 1.03 m diameter was used in the experiments with the same cohesive sediments from fish food. A complete system for water recirculation (**Figure 1**) was implemented. Water is obtained by a high rise tank with a constant water level in order to supply a constant flow rate by using gravity. Diffusers at different levels on the tank wall control the flow rate and tank water velocity, together with the generation of the circular flow. A settling device in the center of the tank allows solids removal.

Using this recirculation tank settling velocities and sizes of sediments were obtained from commonly used fish food and excreta coming from experimental station El Zarco, which cultivates trout. It is owned by Semarnap, the Mexican state agency of environment, natural resources, and fisheries, and is located at 2800 masl in Salazar Estado de México, México.

The next stage consisted to analyze suspended cohesive sediments coming from the Usumacinta and Grijalva rivers in México. In order to reproduce hydrodynamic conditions prevailing in the river and to analyze the flocculation process during long range experiments, an annular rotating flume, 1.3 m diameter and 15×15 cm flume cross section made of Plexiglas, was used (**Figure 2**). The cohesive sediments were analyzed using PTV, during 1.5 h. long experiments and images were taken every 15 min. From this experiment floc sizes and settling velocities were obtained.

2.2. Theoretical settling velocity models

The greatest challenge in the proposal of a settling velocity model for flocs is the adequate definition of their density. Many models have been formulated for floc density [17], in this research the adopted model is the one proposed by Kranenburg [18], as shown in Eq. (2)

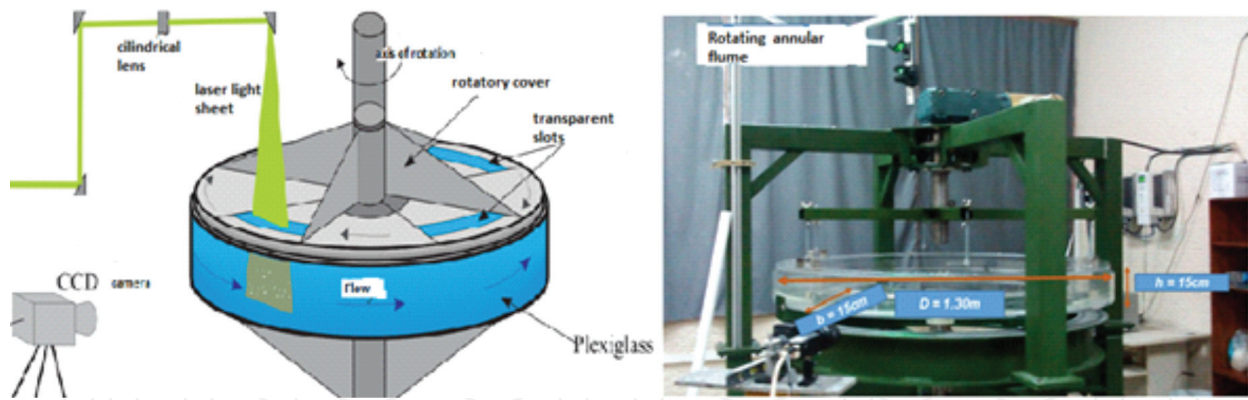


Figure 2. Rotating annular flume and PTV set up.

$$\rho_f - \rho_w = (\rho_p - \rho_w) \left(\frac{D}{d} \right)^{F-3} \quad (2)$$

where ρ_f , ρ_w , and ρ_p are densities of floc, water, and primary particles, respectively, D is the floc diameter and d is the primary particles diameter. F is the fractal dimension and the model assumes that the floc is constituted of spherical primary particles of equal diameter. The model can be used for non-spherical particles with equivalent diameters.

A balance of drag forces and gravitational forces gives Eq. (3)

$$W_s^2 = \frac{4(\rho_f - \rho_w)gD}{3C_{Df}\rho_w} \quad (3)$$

where W_s is the floc settling velocity and C_{Df} is the permeable particle drag coefficient. Using Eqs. (2) and (3), the following relationship for the settling velocity is obtained

$$W_s = \sqrt{\frac{4(S-1)g(D)^{F-2}}{3C_{Df}(d)^{F-3}}} \quad (4)$$

with S is the primary particles relative density.

Using Particle Tracking Velocimetry methods (PTV), Garcia Aragon et al. [19] have shown that a useful relationship for the drag coefficient of a permeable floc has the following form:

$$C_{Df} = \frac{15}{R_{ep}^n} \quad (5)$$

where the coefficient n depends on the kind of floc and varies, according to a comparison of results of different authors [20], between 1.1 and 1.25. R_{ep} is the particle Reynolds number defined as $R_{ep} = W_s D / \nu$ where ν is the kinematic viscosity of the fluid.

Replacing the relationship from Eq. (5) in Eq. (4), the following relationship for the settling velocity is obtained:

$$W_s = \frac{[13.08(S-1)]^{\frac{1}{2-n}} D^{\frac{F+n-2}{2-n}}}{15^{\frac{1}{2-n}} \nu^{\frac{n}{2-n}} d^{\frac{F-3}{2-n}}} \quad (6)$$

where W_s is in m/s and D and d in m.

As the fractal dimension changes with floc diameter, in this paper, we used a relationship proposed by Garcia-Aragon et al. [16] that has a form similar to the following:

$$F = 3 - \alpha \left[\frac{D}{d} \right]^\beta \quad (7)$$

where α and β are constants that depend on the kind of cohesive sediment. Maggi et al. [21] used flocculated kaolinite minerals in experiments in a settling column and found that the exponent β varies between -0.092 and -0.112 .

2.3. Application to suspended load estimation in large rivers

Authors working with the Mississippi river sediment transport Colby [22, 23], realized that the predicted Rouse number was not equal to the measured Rouse number in a series of sampled vertical profiles of the Mississippi. Also, researchers working in the three Gorges Reservoir in the Yangtze River show that settling velocities calculated with diameters obtained from particle size analyzers do not reproduce observed settling velocities, which indicate the existence of flocculation [24]. The formation of flocs in large rivers is the reason why Rouse equation cannot be used with particle sizes from classical granulometric measurements in conjunction with non-cohesive settling velocity equations. Recently, researchers working in the Amazon River and tributaries made similar observations [1]. Their conclusion was that granulometric measurements performed did not represent the real particle size because cohesive sediments agglomerate to form flocs [5, 6, 9] and after sampling, these flocs are destroyed and could not be measured appropriately in laboratory. On a related note, other researchers have shown that particle sizes in the Amazon River are lower than $70 \mu\text{m}$ [25, 26], which are in the size range of cohesive sediments.

To estimate the suspended sediment profile in stationary flows, the following Rouse equation is generally accepted [27]

$$\left(\frac{C(y)}{C(a)} \right) = \left(\frac{H-y}{y} \cdot \frac{a}{H-a} \right)^{Z_R} \quad (8)$$

where the Rouse parameter is $Z_R = W_s/Ku^*$, $C(y)$ is the suspended sediment concentration at height y above bed, H is flow depth, a is a reference depth above bed, and K is Von-Karman's constant that for low sediment concentration is equal to 0.41 .

In this project, Eq. (6) is used to estimate the settling velocity W_s , in conjunction with the Rouse Eq. (8) for the evaluation of the suspended sediment profiles in the Grijalva and Usumacinta rivers, the two largest rivers in Mexico.

2.4. Application of digital holography for PIV (DHPIV) for cohesive sediments characterization

Even if there are enormous advances in PIV and PTV techniques, there are shortcomings for 2D applications. The latter is observed in some physical phenomena, for example for the volume determination of a floc, which is only possible with 3D optical techniques. One of these techniques is digital holography for particle image velocimetry (DHPIV). This technique has been shown appropriate, for size distribution, volume determination, and particle velocity in fluids [30].

The DH method consists of specific steps as shown in **Figure 3**. Most experiments in scientific literature record a hologram following the so called in line system [28–30]. In this configuration, a coherent and collimated laser beam is sent, this is divided in two beams, one is directed toward the particles suspended in the fluid and is called the reference beam, while the dispersed light is called object beam. The two beams interfere to form a hologram which is recorded by the CCD digital camera (**Figure 3**). A typical particle hologram contains a succession of circular concentric interference strips which define the object in three dimensions.

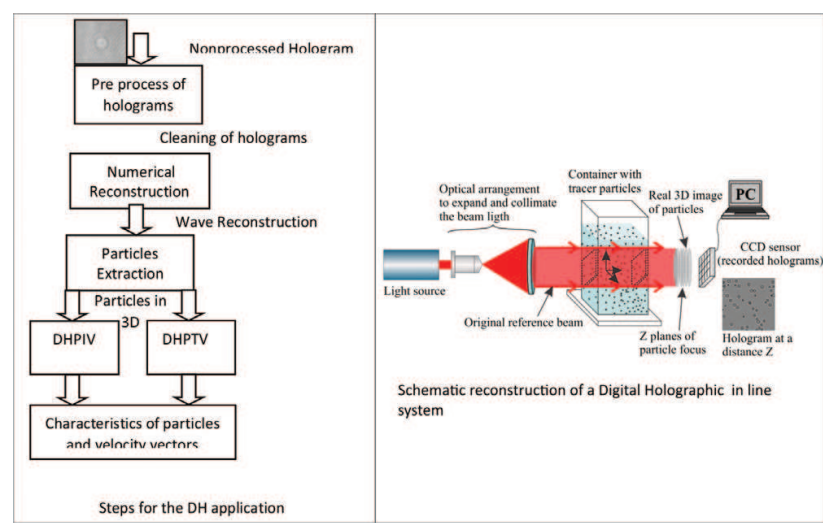


Figure 3. In line digital holographic system.

Green light laser diode	532 nm wave length, 50 mW power
Microscope objective	40×
Pinhole to expand and collimate beam	10 and 5 μm
Lens to collimate the wave front	Focal distance f = 75 mm, 7 cm diameter
Polarizing filters	
Glass container	5 × 5 × 10 cm, glass width 3 mm
Digital camera Lumenera	100 fps, pixel size Dx = Dy = 5.2 μm, 1200 × 1400 px
Sample of fluid to analyze	

Table 1. Physical components of digital holographic system.

For application and calibration of a DH optical system, cohesive sediments from a waste water plant were used. A coagulant was added in order to allow floc formation in the rotating annular flume.

The physical components of the digital holographic system used are described in **Table 1**.

Holographic images acquired and improved are reconstructed numerically in order to obtain 3D characteristics of flocs. The Fresnel method was used for image reconstruction [31].

3. Results

3.1. Experiments with cohesive sediments coming from food for fish

A first analysis of particles coming from fish food, using a Coulter counter analyzer, which destroys flocs, is shown below. The pellets were previously sieved and only those passing sieve 200 (0.075 mm) were conserved. It is observed (see **Figure 4**) that an average diameter of primary particles is 28 μm .

Using the same fish food sediments optical methods were developed in a sedimentation tank. The following settling velocities were obtained at 60 cm from the top of the sedimentation tank by using PTV. It is observed in **Table 2** that the settling velocity increases until a certain value ($D = 200 \mu\text{m}$) and then decreases for larger floc diameters. This behavior is not reflected in classical settling velocity models.

3.2. Experiments with real flocs from an aquaculture recirculation tank

Next long-term experiments were performed in a reduced model of an aquaculture recirculation tank (**Figure 1**), flocs diameters and the corresponding settling velocities were measured for different times using PTV. The sediments used were real flocs coming from a large aquaculture recirculation tank (El Zarco). Some selected samples of the experiments were analyzed by Transmission Electron Microscopy (TEM) (**Figure 5**), at the beginning of the experiment ($t = 0$),

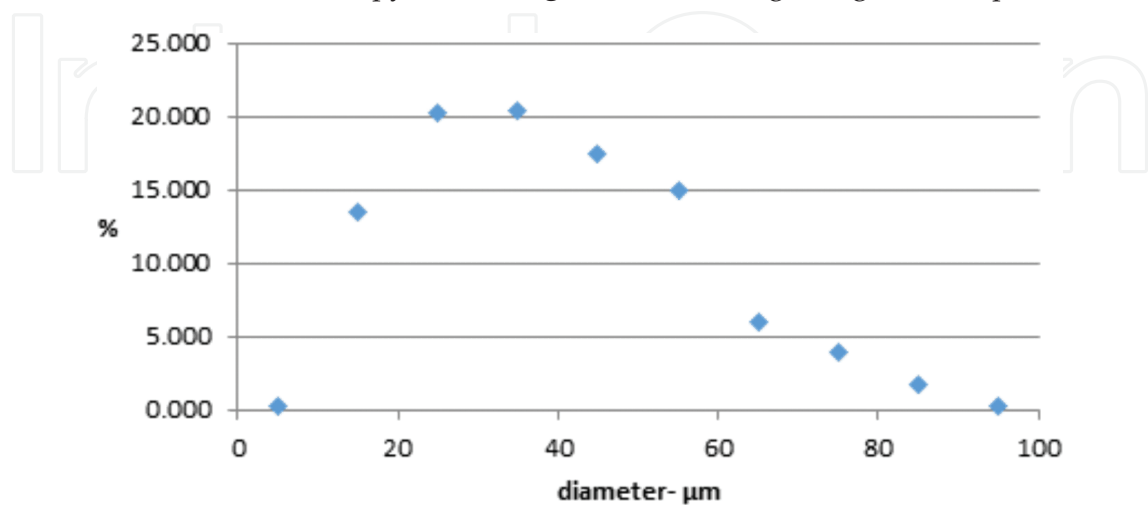


Figure 4. Fish food particle sizes from coulter counter (LS 100Q) analysis.

Floc size	75	100	150	200	250	300	350	400
Ws (cm/s)	0.51	0.62	0.68	0.8	0.79	0.74	0.66	0.54

Table 2. Average settling velocities for fish food in a sedimentation tank (cm/s).

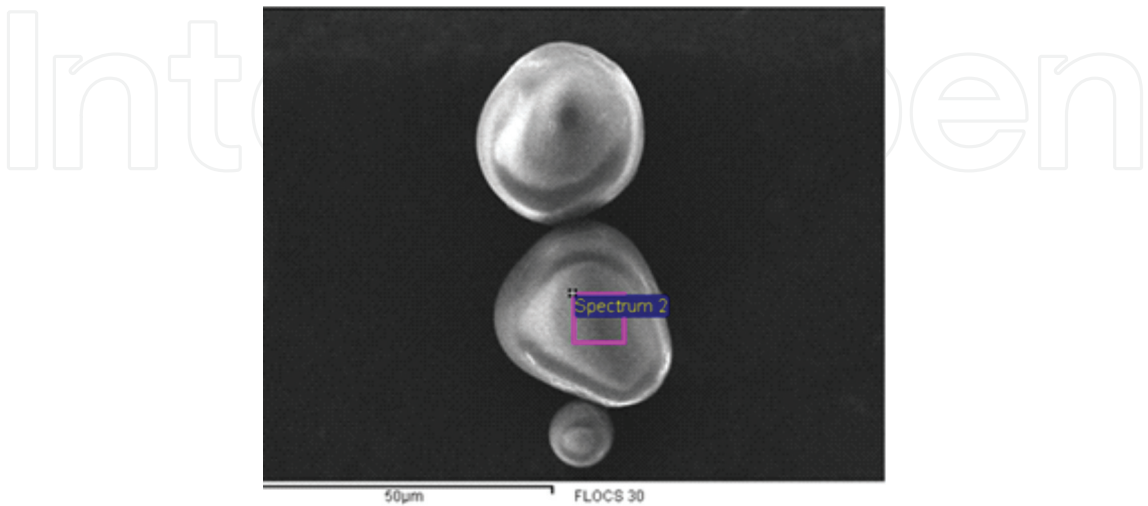


Figure 5. Representative values of fish food primary particles obtained by TEM.

at 15 min ($t = 15$), at 45 min ($t = 45$) and at 1 h ($t = 60$). An average diameter of primary particles of $28\text{ }\mu\text{m}$ was confirmed. Thus, this result was used in the statistical analysis.

In the experiments using the reduced model of an aquaculture recirculation tank, Eqs. (6) and (7) were used for the statistical analysis in order to define the parameters n , α and β . These parameters were defined according to the best correlation coefficient in the relationships W_s vs. D and F vs. D/d . **Figure 6** shows the best fit of F vs. D/d according to Eq. (7). **Table 3** shows the values of α and β obtained at each time.

The average value for the coefficient α was 0.077 and the average value of the coefficient β was 0.726. The latter exponent value is larger than the one obtained by [22] for a similar model, which can be explained with the structure of aquaculture flocs compared to Kaolinite, which is completely different.

Figure 7a–d shows the best fit relationship between W_s and D using the F vs. D/d relationship previously obtained. The resulting n values at different time steps are specified in **Table 4**.

Table 4 shows that the value of n increases as the time of the experiment increases. This observation can be related to the increasing loss of density of the floc. As time increases, the flocs are increasing their volume absorbing water. The latter has two implications; the drag coefficient decreases because the floc becomes more porous and its density decreases.

An interesting feature observed in **Figure 7a–d** is that the settling velocity of the flocs increases for values of floc diameter up to $600\text{ }\mu\text{m}$ and then decreases as floc diameter continues to increase. The settling velocity model proposed in this research is able to reproduce this behavior.

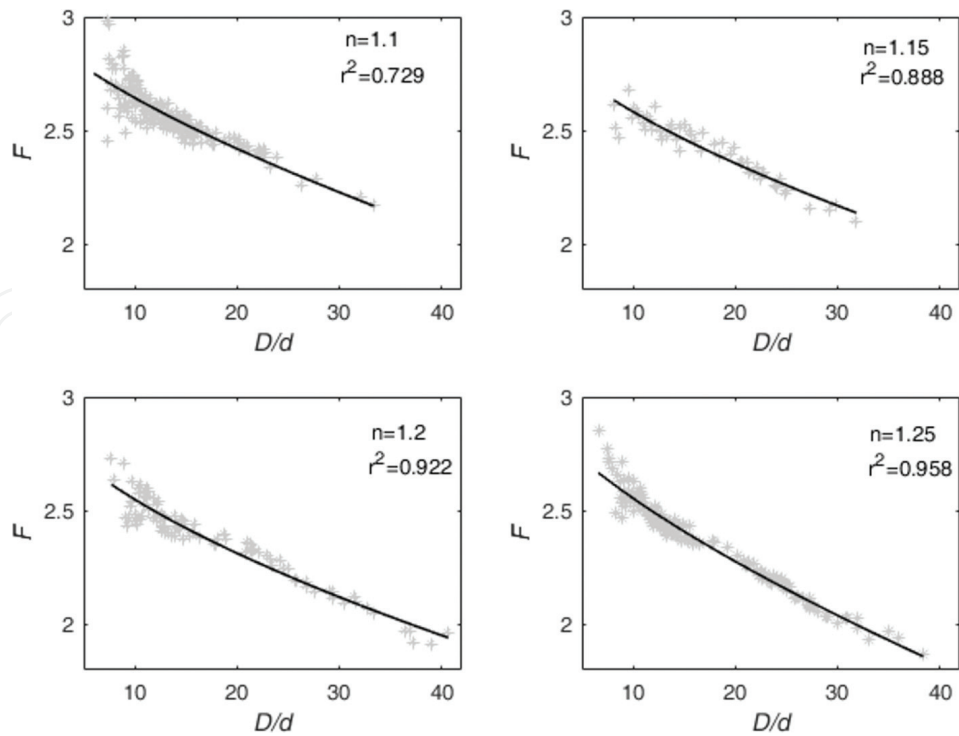


Figure 6. Fractal dimension vs. D/d : (a) at time 0 (upper left), (b) at time 15 min (upper right), (c) at time 45 min (lower left), and (d) at time 60 min (lower right).

Time (min)	α	β
0	0.070	0.703
15	0.049	0.863
45	0.111	0.609
60	0.077	0.727

Table 3. Best fit coefficients for the relationship F vs. D .

This behavior has been shown to occur in nature for different kind of flocs, coming from estuaries, waste water treatment plants, and rivers [10, 19]. Most of the settling velocity models for cohesive sediments show an increase of settling velocity for all diameters which is not observed in this research. The larger flocs are formed after a long experimental period. In **Figure 7a** and **b**, there are few flocs larger than 600 μm , which is not the case for experimental periods of 45 and 60 min (**Figure 7c** and **d**). The practical implication of this phenomenon for aquaculture recirculation tanks is that residence times should not be very long because the larger flocs formed are even more difficult to settle down.

3.3. Experiments with suspended cohesive sediments of Grijalva and Usumacinta rivers

A sampling of suspended cohesive sediments in the Grijalva and Usumacinta rivers was done during high river level on the month of December 2016. The sampling location for the Grijalva

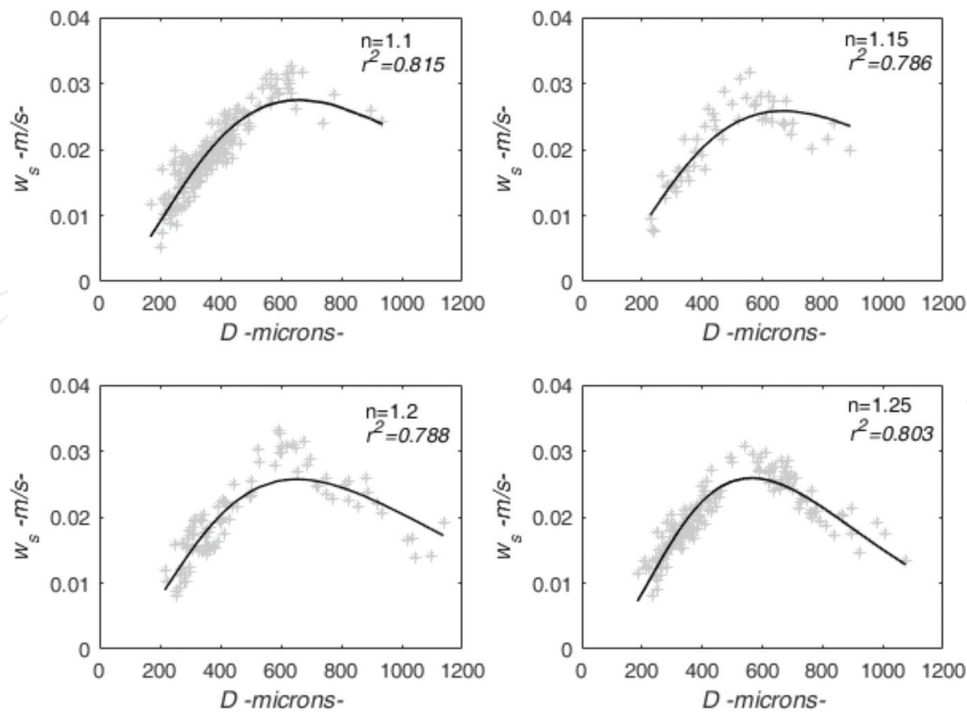


Figure 7. Settling velocity vs. D : (a) at time 0 (upper left), (b) at time 15 min (upper right), (c) at time 45 min (lower left), and (d) at time 60 min (lower right).

Time (min)	n
0	1.1
15	1.15
45	1.2
60	1.25

Table 4. Values of n for best fit relationship between W_s vs. D .

was located before the junction with the Usumacinta, and in the Usumacinta, it was located 20 km upstream of the junction with the Grijalva. Samples were obtained at three vertical water columns in each cross section. For the Grijalva River, the samples were obtained at levels varying from 0.5 to 11 m (maximum water depth) each 1 m. At the Usumacinta River, samples were obtained at levels varying from 0.5 to 17 m (maximum water depth) each 1 m. **Figures 8 and 9** show the suspended sediment concentration profiles for the Grijalva and Usumacinta Rivers, respectively. In these figures, the vertical axis refers to the level z adimensionized with the flow depth H , while the horizontal axis refers to the ratio of the concentration C to a reference concentration C_a .

An average value of Rouse parameter $Z_R = 0.214$ was obtained in the Grijalva River, which is representative of a small increase of suspended sediment charge near the bottom.

An average value of $Z_R = 0.069$ was obtained in the Usumacinta river. This value is representative of near constant suspended sediment charge in the water column.

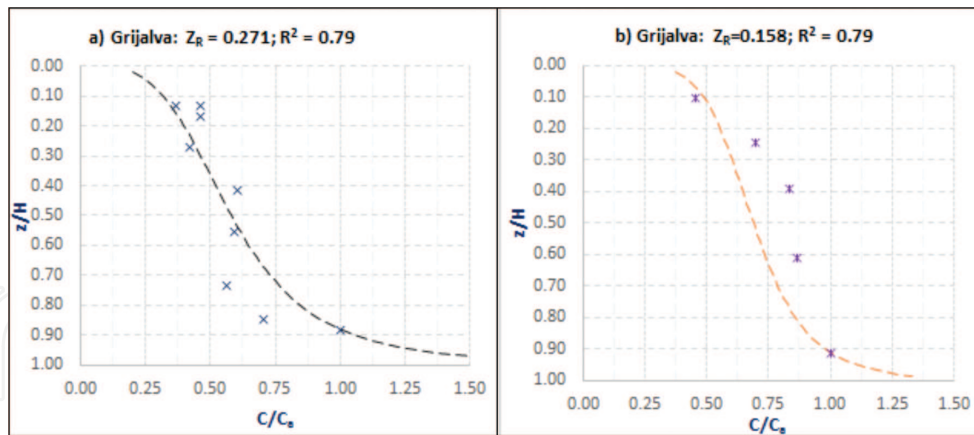


Figure 8. Suspended sediment concentration profiles for the Grijalva River. (a) 55 m from left bank and (b) 90 m from left bank.

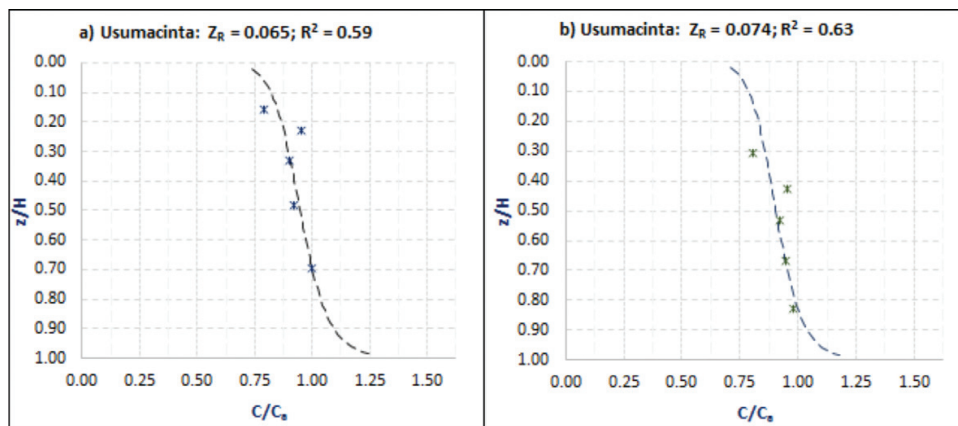


Figure 9. Suspended sediment concentration profiles for Usumacinta river. (a) 25 m from left bank and (b) 140 m from left bank.

Experiments in the rotating annular flume using 50 L samples for the Grijalva and Usumacinta rivers were performed at shear rates similar to those encountered in the field. **Table 5** shows the values of shear velocity (u_*) obtained in the sampling stations of the Grijalva (width 180 m) and Usumacinta (width of 340 m) rivers. The value of u_* was obtained by the horizontal u' and vertical fluctuating velocities w' ($u_*^2 = \overline{u'w'}$), where the over bar indicates an average over the water depth. The velocities were measured the same day of suspended sediment sampling with an Acoustic Doppler Current profiler (ADCP).

Images of flocs after experimental runs of 1.5 h in the Grijalva river samples and 3.5 h in the Usumacinta river samples, in the annular flume using PTV, gave us an average size of flocs of 307 μm in the Grijalva and 209 μm in the Usumacinta. **Table 6** shows the statistical values of flocs obtained in large runs at a shear velocity $u_* = 0.070$ m/s (the average value in the Usumacinta river see **Table 5**) and **Table 7** at $u_* = 0.043$ m/s (the average value at the Grijalva river, see **Table 5**).

Also, microscopic images of some representative flocs were obtained with $40\times$ magnification. An average value of primary particle, after a statistical analysis of 50 flocs images for each

River	Distance from left bank (m)	u_* (m/s)
Grijalva	55	0.048
	90	0.045
	195	0.036
Usumacinta	25	0.064
	140	0.082
	210	0.065

Table 5. Shear velocity in Usumacinta and Grijalva rivers.

Time (min)	D (μm)	Number of data
5	217	33,200
20	188	17,254
50	172	21,542
120	164	12,232
150	242	32,560
180	247	25,441
210	232	23,450
Mean	209	

Table 6. Average floc size at the Usumacinta River from PTV experiments in the rotating annular flume.

Time (min)	D (μm)	Number of data
0	306	33,434
5	308	25,550
20	313	22,652
50	311	21,321
85	297	23,460
Mean	307	

Table 7. Average floc size at the Grijalva River from PTV experiments in the rotating annular flume.

river, gave an estimated value of $1.2 \mu\text{m}$ for the Grijalva river and $3.8 \mu\text{m}$ for the Usumacinta. Two representative images are shown in **Figures 10** and **11**.

When Eq. (6) is used along with the already found average values of D and d, the values of settling velocity are obtained for different floc sizes (**Table 8**) using Eq. (7), with values of $\alpha = 0.07$ and $\beta = 0.72$. The values of S were 1.29 for the Usumacinta river and 1.55 for the Grijalva river. Different values of n (**Table 8**) were used to show the sensitivity of the model to this compaction index.

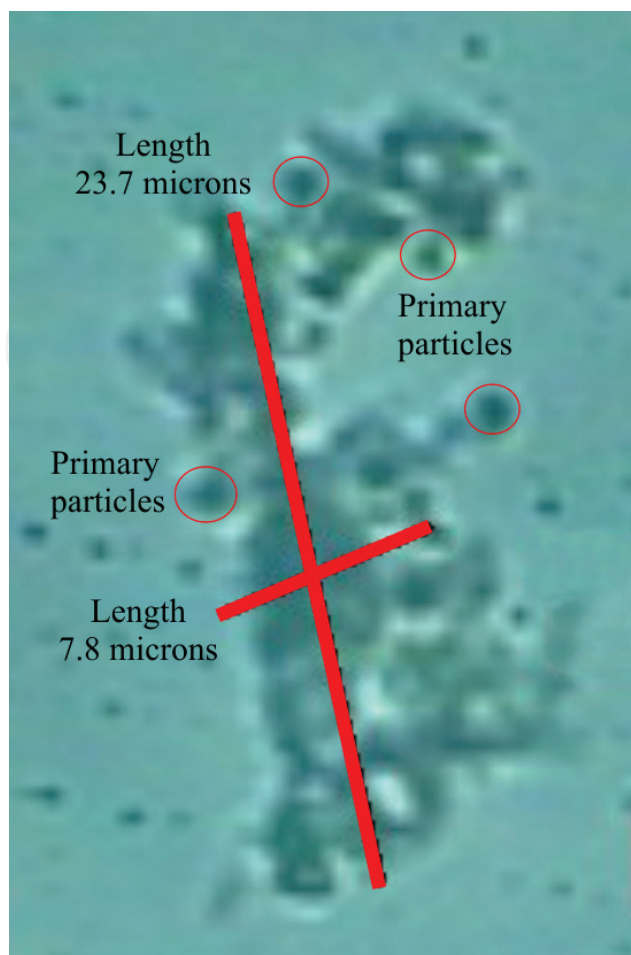


Figure 10. Primary particles and flocs representative of the Grijalva river.

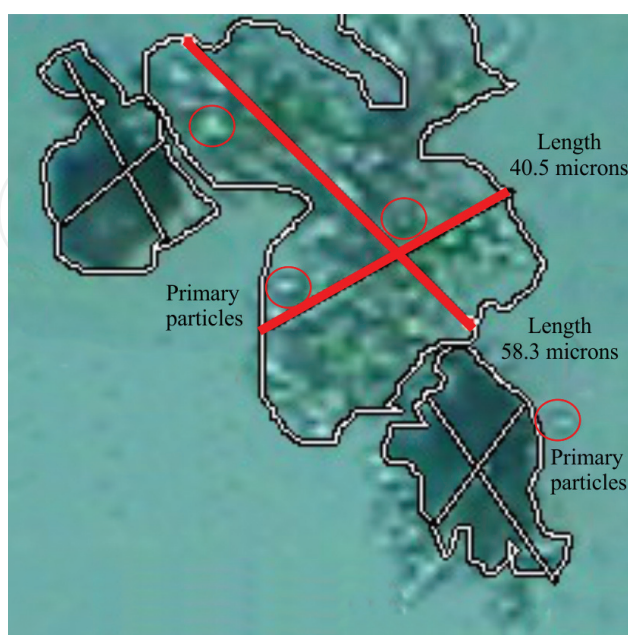


Figure 11. Primary particles and flocs representative of the Usumacinta river.

Table 8 shows that the best estimation of Z_R for the Usumacinta river is obtained with $n = 1.1$ because the average measured Z_R (see **Figure 8**) was $Z_R = 0.069$. Similarly, the best estimation of Z_R for the Grijalva river is also obtained with $n = 1.1$ because the average measured Z_R (see **Figure 9**) was $Z_R = 0.214$. The larger concentrations near the bottom for the Grijalva river are explained by the larger size of flocs in this river ($307 \mu\text{m}$ compared to $209 \mu\text{m}$ for the Usumacinta).

These results indicate that flocs of both rivers are strong flocs (low values of n), which is logical because shear rates at the Usumacinta and Grijalva rivers are high (for comparison u^* at Amazon River varies between 0.07 and 0.1 [1]). It is also observed that the value of Z_R in the Usumacinta river is more sensitive to changes in the value of n . It was observed that for large depths it is more difficult to define the n value as it can change even in the same cross section of the river at different levels.

3.4. Experiments using digital holography for PIV

Figure 12 shows the hologram reconstruction of a spherical particle of $50 \mu\text{m}$. **Figure 12a** shows the particle's hologram already filtered, where the different patterns of diffraction are observed; **Figure 12b** provides greater detail. The relative intensity profile (I/I_{max}) vs. reconstruction distance (z) is shown in **Figure 12c**. The maximum intensity is shown where the particle is in focus.

Figure 13a shows the digital hologram of flocs, while **Figure 13b** shows a preprocess in order to avoid noise in the hologram. Rings of interference are observed in both figures, which define the 3D characteristics of the flocs. **Figure 13c** shows the reconstruction of the binary image. This image only shows the particles that are in the best focus, i.e., where the shape of the particle is clearly defined. In order to find the position in the plane, the diameter, and shape of

n	Ws (mm/s)		Z_R	
	Usumacinta	Grijalva	Usumacinta	Grijalva
1.1	0.19	3.84	0.07	0.223
1.15	0.16	3.87	0.05	0.225
1.2	0.13	3.91	0.04	0.227
1.25	0.10	3.95	0.03	0.229

Table 8. Estimated values of W_s and corresponding values of Z_R .

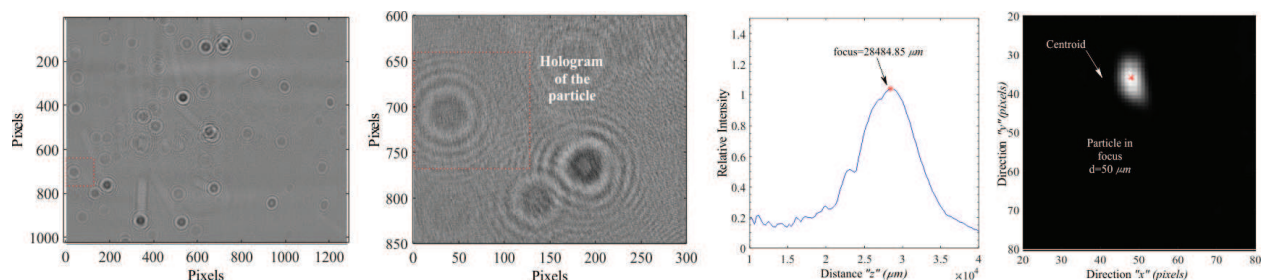


Figure 12. Results of a reconstruction of hologram process. (a) Originally filtered hologram; (b) one particle hologram; (c) relative intensity profile, and (d) reconstructed particle.

the particle, the PTV algorithm for non-spherical particles was applied. **Figure 13d** shows particles pair detection and its centroid, which allows us to determine particles' velocity for a sequence of holograms.

A settling column was used in order to observe the hologram evolution over time. Almost 100 holograms were processed each recording time. The times recorded were $t = 0, 10, 20, 30, 45$, and 60 min. **Figure 14a** shows particles distribution for holograms at time $t = 0$, and it can be observed that maximum size is 160 μm , with a mean diameter of 70 μm .

Figure 14c shows the distribution of particles at time 30 min, where an increase in size of flocs is observed attaining a maximum of 180 μm and a mean value of 80 μm . It is also observed that the shape of the distribution is log-normal, similar to theory. **Figure 14d** shows clearly a non-uniform distribution of particles in a hologram.

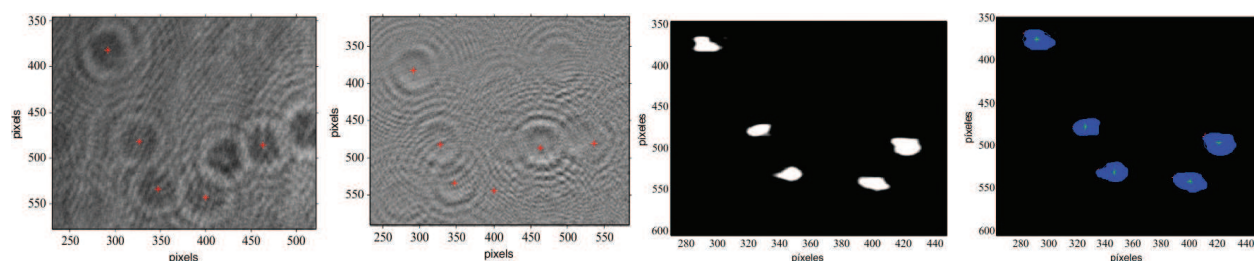


Figure 13. Results of analysis of a digital hologram. (a) Original digital hologram; (b) processed digital hologram; (c) reconstructed hologram, and (d) size and shape of detected particles.

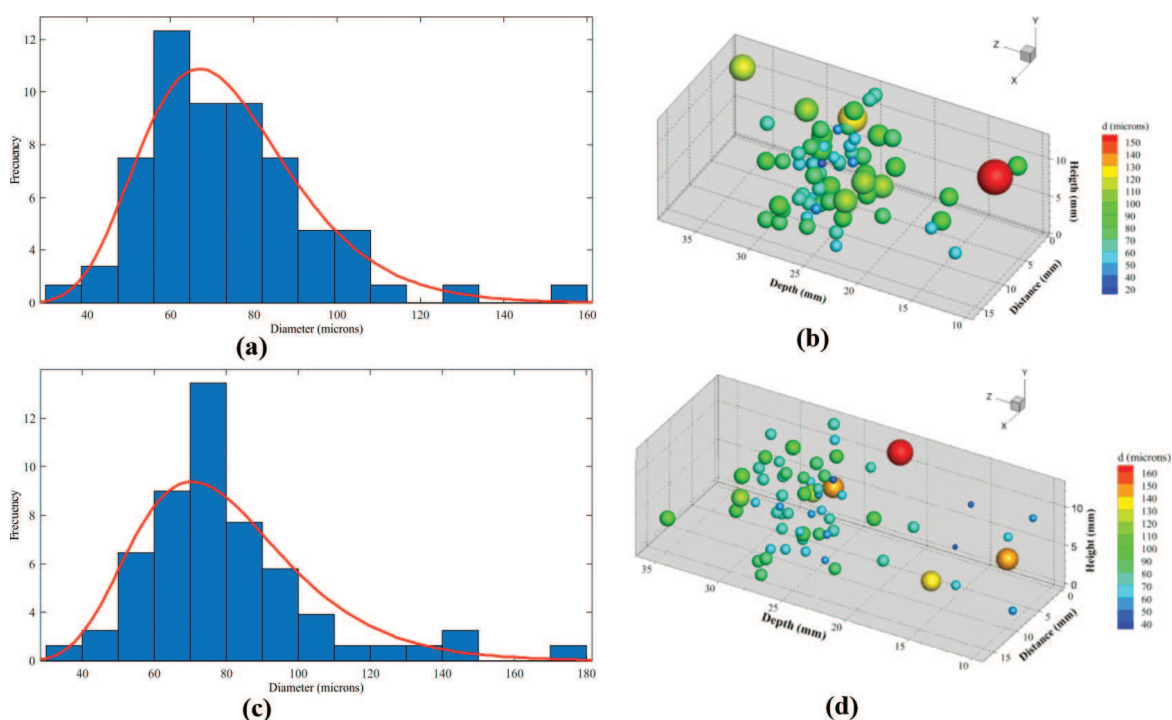


Figure 14. Characteristics of flocs in settling column (a) frequency distribution of sizes at $t = 0$ min; (b) spatial distribution of flocs at $t = 0$ min; (c) frequency distribution of sizes $t = 30$ min; (d) spatial distribution of flocs at $t = 30$ min.

4. Conclusions

A model to estimate the floc settling velocity was calibrated for flocs obtained from aquaculture recirculation tanks that cultivate trout. The model was able to reproduce the values of settling velocity which varies between 0.01 and 0.025 m/s. For all the recording times analyzed there is a maximum settling velocity for flocs of diameter of 600 μm .

The representative values of the parameters used to determine fractal dimension are proposed in this research according to the experimental results. These values depend on floc density and vary with experimental time as flocs become more porous. The values found in this research apply to flocs coming from trout cultures in high level locations, i.e., 2800 masl.

The practical findings for aquaculture recirculation tanks design is that residence times should be short in order to minimize the presence of very large flocs. Middle size flocs settle faster. In designing the central settling device, which functions according to the hydrocyclons principle, the up flow velocity should be less than 0.01 m/s in order to diminish the flow of sediments toward the recirculation deposit.

A method to obtain the suspended sediment concentration profiles for rivers with mainly cohesive sediments was presented. It is necessary to take some representative samples and using a rotating annular flume defines a steady state of flocculation after long-term runs. The most suitable method to analyze size and settling velocity of flocs are optical methods, PTV and microscopy. This research shows that the settling velocity can be accurately calculated with Eq. (6) in order to obtain an appropriate estimation of the Rouse number Z_R . This allows us to properly determine the suspended sediment concentration profiles in rivers carrying a large amount of cohesive sediments.

Non-intrusive optical techniques are a suitable tool to characterize cohesive sediments, because they do not destroy flocs and allow for microscopic analysis. More advanced optical methods, like DHPIV, are showing good results for floc size and shape determination, thus in the future they will be the best method for cohesive sediment analysis.

Author details

Juan Antonio Garcia Aragon*, Salinas Tapia Humberto, Diaz Palomarez Victor and Klever Izquierdo Ayala

*Address all correspondence to: jagarciaa@uaemex.mx

CIRA-Faculty of Engineering, Universidad Autónoma del Estado de México, Toluca, Mexico

References

- [1] Bouchez J, Metivier F, Lupker M, Maurice L, Perez M, Gaillardet J, France-Lanord C. Prediction of depth-integrated fluxes of suspended sediment in the Amazon River: Particle aggregation as a complicating factor. *Hydrological Processes*. 2011;**25**:778-794

- [2] Mikkelsen OA, Milligan T, Hill P, Moffatt D. INSSECT—An instrumented platform for investigating floc properties close to the seabed. *Limnology and Oceanography: Methods*. 2004;**2**:226-236
- [3] Nimmo Smith WAM, Atsavapranee P, Katz, Osborn TR. PIV measurements in the bottom boundary layer of the coastal ocean. *Experiments in Fluids*. 2002;**33**:962-971
- [4] Wheaton FW. *Aquaculture Engineering*. New York: Wiley-Interscience; 1977. p. 708
- [5] Droppo IG. Rethinking what constitutes suspended sediment. *Hydrological Processes*. 2001;**14**:653-667
- [6] Droppo IG, Ongley ED. Flocculation of suspended sediment in rivers of south-eastern Canada. *Water Research*. 1994;**28**:1799-1809
- [7] Nicholas AP, Walling DE. The significance of particle aggregation in the overbank deposition of suspended sediment on river floodplains. *Journal of Hydrology*. 1996;**186**:275-293
- [8] Droppo IG. Suspended sediment transport-Flocculation and particle characteristics. In: Anderson MG, editor. *Encyclopedia of Hydrological Sciences*. New Jersey, USA: John Wiley & Sons, Ltd; 2005
- [9] Garcia-Aragón J, Droppo I, Krishnappan B, Trapp B, Jaskot C. Erosional characteristics and floc strength of Athabasca river cohesive sediments. *Journal of Soils and Sediments*. 2011;**11**(2):679-689
- [10] Khelifa A, Hill PS. Models for effective density and settling velocity of flocs. *Journal of Hydraulic Research*. 2006;**44**(3):390-401
- [11] Maggi F. The settling velocity of mineral, biomineral, and biological particles and aggregates in water. *Journal of Geophysical Research, Oceans*. 2013;**118**(4):2118-2132
- [12] Maggi F, Tang FH. Analysis of the effect of organic matter content on the architecture and sinking of sediment aggregates. *Marine Geology*. 2015;**363**:102-111
- [13] Watten BJ, Beck LT. Comparative hydraulics of rectangular cross flow rearing unit. *Aquaculture Engineering*. 1987;**6**:127-140
- [14] Summerfelt SG, Wilton G, Roberts D, Rimmer T, Fonkalrsrud K. Developments in recirculating systems for arctic char culture in North America. *Aquacultural Engineering*. 2004;**30**:31-71
- [15] Timmons M.B., Summerfeld S.T. y Vinci B.J. Review of circular tank technology and management. *Aquacultural Engineering* 1998;**18**:51-69
- [16] Garcia-Aragon JA, Droppo I, Krishnappan B, Trapp B, Jaskot C. Experimental assessment of Athabasca River cohesive sediment deposition dynamics. *Water Quality Research Journal of Canada*. 2011b;**46**(1):87-96
- [17] Li DH, Ganczarczyk JJ. Stroboscopic determination of settling velocity, size and porosity of activated sludge flocs. *Water Research*. 1987;**21**(3):157-262

- [18] Kranenburg C. The fractal structure of cohesive sediment aggregates. *Estuarine, Coastal and Shelf Science*. 1994;**39**:1665-1680
- [19] Garcia-Aragon JA, Salinas-Tapia H, Moreno-Vega J, Diaz-Palomarez V, Tejeda-Vega S. A model for the settling velocity of flocs; application to an aquaculture recirculation tank. *International Journal of Computational Methods and Experimental Measurements*. 2014;**2**(3):313-322. DOI: 10.2495/CMEM-V2-N3-313-322
- [20] Johnson CP, Xiaoyan LI, Logan BE. Settling velocities of fractal aggregates. *Environmental Science & Technology*. 1996;**30**:1911-1918
- [21] Maggi F, Mietta F, Winterwerp JC. Effect of variable fractal dimension on the floc size distribution of suspended cohesive sediment. *Journal of Hydrology*. 2007;**343**:41-55
- [22] Jordan PR. Fluvial sediment of the Mississippi River at St. Louis, Missouri. USGS Water-Supply Paper No. 1802. <http://pubs.er.usgs.gov/djvu/WSP/wsp 1802.djvu>. 1965
- [23] Scott CH, Stephens HD. Special sediment investigations: Mississippi river at St. Louis, Missouri, 1961–1963. 1966. USGS Water-Supply Paper No. 1819-J. <http://pubs.er.usgs.gov/djvu/WSP/wsp 1819-J.djvu>
- [24] Li W, Wang J, Yang S, Zhang P. Determining the existence of the fine sediment flocculation in the three gorges reservoir. *Journal of Hydraulic Engineering*. 2015;**141**(2):05014008
- [25] Meade RH, Nordin CF, Curtis WF. Sediment in Rio Amazonas and some of its principal tributaries during the high water seasons of 1976 and 1977. In: *Proceedings of the III Simposio Brasileiro de Hidrologia (Brasília)*; Vol. 2; ABRH; Brazil; 1979. pp. 472-485
- [26] Meade RH. Suspended sediment in the Amazon River and its tributaries in Brazil, during 1982–1984. US Geol. Survey Open File Report 85-492. US Geol. Survey, Denver, Colorado, USA. 1985
- [27] Chien N, Wan Z. *Mechanics of Sediment Transport*. Reston, Virginia, USA: ASCE Press; 1999. p. 913
- [28] Vikram CS. *Particle Field Holography*. Cambridge, UK: Cambridge University Press; 1992
- [29] Satake S, Kunugi T, Sato K, Ito T. Digital holographic particle tracking velocimetry for 3-D transient flow around an obstacle in a narrow channel. *Optical Review*. 2004;**11**: 162-164
- [30] Sheng J, Malkiel E, Katz J, Adolf J, Belas R. Digital holographic microscopy reveals prey-induced changes in swimming behavior of predatory dinoflagellates. *Proceedings of the National Academy of Sciences*. 2007;**104**(44):17512-17517
- [31] Schnars U, Jüptner W. *Digital Holography: Digital Hologram Recording, Numerical Reconstruction, and Related Techniques*. Berlin Heidelberg: Springer; 2005

